AD-A157 718 THE SPACING OF RED CELLS IN THE MICROCIRCULATION DURING ACUTE ANEMIA(U) NAVAL MEDICAL RESEARCH INST BETHESDA MD L D HOMER ET AL. SEP 84 NMRI-84-55 1/1

UNCLASSIFIED F/G 6/16 NL

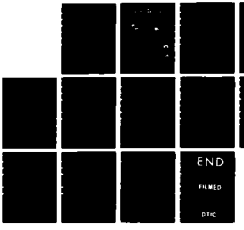

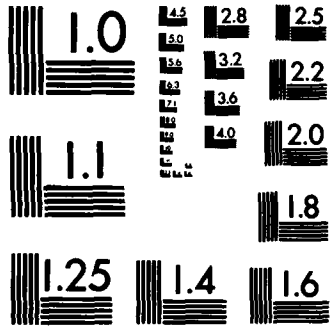

MICROCOPY RESOLUTION TEST CHART
NATIONAL BUREAU OF STANDARDS-1963-A

NAVAL MEDICAL RESEARCH INSTITUTE
BETHESDA, MARYLAND

84-55

THE SPACING OF RED CELLS IN
THE MICROCIRCULATION DURING ACUTE ANEMIA.

L.D.HOMER, J.B.SHELTON AND H.MCELROY

R.L. SPHAR, CAPT, MC, USN
Commanding Officer
Naval Medical Research Institute

NAVAL MEDICAL RESEARCH AND DEVELOPMENT COMMAND

ACKNOWLEDGEMENTS

We thank Ms. Julie Crockett for the capable assistance she has given us in editing and revising successive drafts of this manuscript.

The experiments conducted herein were conducted according to the principles set forth in the "Guide for the Care and Use of Laboratory Animals," Institute of Laboratory Animal Resources, National Research Council, DHEW Pub. (NIH) 78-23.

This research was supported by Naval Medical Research and Development Command, Research Work Unit No. MR0410106.0001. The opinions and assertions contained herein are the private ones of the writers and are not to be construed as official or as reflecting the views of the Navy Department or the naval service at large.

UNCLASSIFIED

SECURITY CLASSIFICATION OF THIS PAGE (When Data Entered)

REPORT DOCUMENTATION PAGE		READ INSTRUCTIONS BEFORE COMPLETING FORM
1. REPORT NUMBER NMRI 84-55	2. GOVT ACCESSION NO. AD-A167	3. RECIPIENT'S CATALOG NUMBER 718
4. TITLE (and Subtitle) THE SPACING OF RED CELLS IN THE MICROCIRCULATION DURING ACUTE ANEMIA		5. TYPE OF REPORT & PERIOD COVERED Medical Research Progress Report, Final 6. PERFORMING ORG. REPORT NUMBER
7. AUTHOR(s) LOUIS D. HOMER, JOSEPH B. SHELTON and HOWARD MCELROY		8. CONTRACT OR GRANT NUMBER(s)
9. PERFORMING ORGANIZATION NAME AND ADDRESS Naval Medical Research Institute Bethesda, Maryland 20814		10. PROGRAM ELEMENT, PROJECT, TASK AREA & WORK UNIT NUMBERS MR0410106.0001 Report No.3 61153N
11. CONTROLLING OFFICE NAME AND ADDRESS Naval Medical Research & Development Command Bethesda, Maryland 20814		12. REPORT DATE September 1984 13. NUMBER OF PAGES 28
14. MONITORING AGENCY NAME & ADDRESS(if different from Controlling Office) Naval Medical Command National Capital Region Bethesda, Maryland 20814		15. SECURITY CLASS. (of this report) Unclassified 15a. DECLASSIFICATION/DOWNGRADING SCHEDULE

16. DISTRIBUTION STATEMENT (of this Report)

Approved for public release and sale. Distribution unlimited

17. DISTRIBUTION STATEMENT (of the abstract entered in Block 20, if different from Report)

18. SUPPLEMENTARY NOTES

NMRI Report. September 1984.

19. KEY WORDS (Continue on reverse side if necessary and identify by block number)

oxygen transport, hypoxia, shunting, cardiac output regulation

micrometers

20. ABSTRACT (Continue on reverse side if necessary and identify by block number)

When rats are made acutely anemic by replacing blood with solutions of albumin and salts, detectable gaps between red cells in capillaries increase in size from 4.44±.63 μm at a hematocrit of 0.4, to 11.3±3.7 μm at a hematocrit of 0.1. At low hematocrits, cells appear to occupy a smaller fraction of the capillary cross section (.222±.022 at a hematocrit of 0.1) than at higher hematocrits (.442±.014 at a hematocrit of 0.4). The size of plasma gaps is not uniform, but so variable that cell-free plasma spaces as large as 12 μm

(continued on back)

DD FORM 1 JAN 73 1473 EDITION OF 1 NOV 65 IS OBSOLETE
S/N 0102-LF-014-6601

UNCLASSIFIED

SECURITY CLASSIFICATION OF THIS PAGE (When Data Entered)

Continuation of block 20.

are relatively common even at a hematocrit of 0.4. Gaps of this size could give rise to plasma PO_2 tensions 20 mm Hg lower than red cell PO_2. Such gradients are large enough to be detected by optical methods and suggest to us the possibility that plasma gaps may play a role in the regulation of blood flow.

TABLE OF CONTENTS

List of Tables iii

List of Illustrations iv

Introduction 1

Methods 2

Analytical Methods 5

Results 8

Plasma Spaces Between Cells 9

Discussion 16

References 22

LIST OF TABLES

Table 1. Parameters of maximum likelihood estimates

Table 2. Maximum likelihood estimates and standard errors

LIST OF ILLUSTRATIONS

Figure 1. Fraction of capillary with cell-free gaps

Figure 2. Average length of cell-free gaps

Figure 3. Average length of dark segments

Figure 4. Average square length of cell-free gaps

Figure 5. Maximum drop in oxygen tension in cell-free gaps

INTRODUCTION

During acute anemia, the average distance between red cells necessarily increases. This must be true in the microcirculation as well as in the general vascular spaces. It has been proposed that, as a consequence, there might be regions of hypoxia between red cells passing single file through small vessels (Homer et al., 1981). The degree of hypoxia is determined in part by the length of the spaces between the cells. It was our purpose, in the experiments to be described, to obtain some measurements of the relationship between systemic hematocrit and red cell spacing. We have used these measurements to determine with what degree of anemia one might reasonably expect the occurrence of detectable oxygen gradients.

METHODS

Rats weighing 280 to 395 g were anesthetized by intraperitoneal injection of 0.6 ml/kg of a solution containing 100 mgm/ml of dial and 400 mgm/ml of urethane. A small polyethylene catheter was inserted in the right jugular vein to permit withdrawal of blood or infusion of fluid. A catheter with a thermistor bead mounted on the tip was threaded into the aorta through the left carotid artery. A portion of the tail was shaved with a razor blade, removing old skin until the region was pink and scattered points of bleeding could be seen. The tail so prepared was mounted on a microscope stage and held fixed by its sides. A drop of saline was placed on the shaved skin and

covered with a glass cover slip. The rat was next given 4 ml of a 6% solution of human albumin in Ringer's lactate solution. While this injection was allowed to mix into the rat's circulation for 15 minutes, video recordings of a micrometer scale were made for subsequent calibration and a field suitable for recording was found. We sought capillaries 5 to 10 μm in diameter with vigorous flow, in which it appeared red cells would be forced to travel in single file. Next, duplicate cardiac output determinations were made by thermal dilution. Then a 15-second video recording of the chosen field was made. After this, 4 ml of blood was withdrawn. The last 2 ml were used for the hematocrit measurements. Immediately afterwards, 4 to 4.3 ml of the albumin solution were given and a waiting period allowed to elapse before repeating the cycle of cardiac output measurement, video recording, blood withdrawal, fluid replacement, and a waiting period. Cycles were timed to take 20 minutes all together and were continued until at least one hematocrit measurement fell below 20%.

The arterial thermistor used to determine cardiac output also served to measure body temperature, which was kept near 37° C with a heating pad, supplemented, as necessary, with a light bulb in a gooseneck lamp.

The microscopes used were equipped with a Leitz Ultropak illuminator and a 22X objective with a numerical aperture of .45, or with a 24X objective having a .65 numerical aperture, which was used with a Leitz Ploemopak vertical illuminator. A broad band filter with 60% peak transmission at 400 nm and one-half bandpass of 70 nm was

placed between the microscope objective and the camera tube to enhance contrast between red cells and plasma. The microscope image was focused on the tube of a Cohu 4410/ISIT television camera without an eyepiece or other lens between the objective and the face of the camera tube. The camera signal was passed through a time and date generator and recorded on a Panasonic NV-8030 television tape recorder. A television monitor was used to focus the microscope and select areas appropriate for recording. We used a xenon arc lamp driven by a Strobrite 3015 stroboscope to light the field. While focusing, the flash frequency was adjusted to approximately 60 Hz to match the vertical scanning frequency of the television camera. Recordings were made with the camera auto-gain turned off and the flash running at near 20 Hz, thereby illuminating the field at approximately every third frame. After the experiment, the videotape was played into an Eigen 16-10 video disc, which in turn was connected to an Eyecom II image analyzer interfaced to a DEC PDP 11/40 digital computer.

Our selection of video images for analysis was neither systematic nor completely random. A 10-second segment of the original recording was transmitted to the video disc. Had our flash been synchronized with the vertical retrace of the video signal, 200 of the 600 frames would have been properly exposed. Each of 200 frames following the well-exposed frame would appear badly faded, and the next frame dark. Because our flash frequency was autonomously controlled and only haphazardly synchronous with the camera, many of our frames were

partly dark, partly well-exposed. If the vessel to be studied was so divided, the frame was not used. With this restriction in mind, samples from suitably exposed frames were taken at approximately equal intervals throughout the 10-second recording period, and the sums from multiple frames pooled to give a single set of numbers for each experimental period.

The digitized television picture had a field of 300 to 400 μm in the horizontal direction and a pixel spacing of about 0.5 μm. Calibration factors were not quite the same in the vertical direction as in the horizontal direction, and values reported here have been calculated using interpolations based on separate calibration factors in the two directions. To begin the analysis of the digitized image, a skeleton of the central axis of the vessel being studied was drawn using a cursor controlled by a joystick and an interactive computer program. Once the skeleton had been drawn, the program examined the intensities along a 21-μm line at right angles to the skeleton, and computed the average intensities of the inner 7 μm covering the vessel and the average intensities of an outer 7 μm on either side. If the average in the central 7 μm was 5% darker than the averages on the outside, this was classified as lying over a red cell. Otherwise, it was classified as a plasma space. By moving this line along the length of the vessel, the program compiled the lengths of alternate spaces of light and dark. The sums of light and dark lengths were found, as well as the sum of squared lengths and the number of alternations from light to dark segments. Finally, the program marked its selected

light spaces for visual verification. The only instances in which we found it necessary to reject the program selection occurred when the axis had been poorly marked or had shifted between measurements. By summing lengths from many frames, the total capillary length sampled for each hematocrit determination was never less than 780 μm, with a median sampled length greater than 1500 μm. This algorithm was developed and tested using pilot studies not reported here and gave results agreeing with visual judgments of spacing whenever the spacing was distinct. It provided a consistent procedure, not requiring decisions on the part of the observer, whenever precise location of the transition from a light space to a dark space seemed difficult. It provided a much more rapid analysis than would have been possible with manual measurements.

ANALYTICAL METHODS

For our quantitative analysis we have used several simple ideas relating systemic hematocrit to the lengths of light and dark segments observable in the capillaries. Systemic hematocrit, H, must be, on the average, related to the microvascular cell flow, F_c, and the plasma flow, F_p, by the expression,

$$H = F_c/(F_c + F_p). \qquad [1]$$

Capillary hematocrit will generally be smaller than systemic hematocrit, but the mass flow fraction in the capillary for cells is close to the

systemic hematocrit (Klitzman & Duling, 1979). The sum of the clear spaces between lengths of cells traveling single file through the capillary is L_p, and the sum of the cell lengths is L_c. We assume flow is occurring in a circular section of radius, r, at a linear velocity $\dot{x}$. We also assume that a cell occupies only a fraction, α, of the available cross section. Then,

$$F_c = \alpha\pi r^2 \dot{x} L_c/(L_c + L_p), \quad [2]$$

$$F_p = \pi r^2 \dot{x}(L_c(1 - \alpha) + L_p)/(L_c + L_p). \quad [3]$$

We assume a central plasma velocity that is the same as red cell velocity. According to this model, if a still layer of plasma exists at the periphery, the average plasma velocity would be lower than the observed red cell velocity, and the microvascular hematocrit less than the systemic hematocrit. Using these three equations we may obtain,

$$H = \alpha L_c/(L_c + L_p). \quad [4]$$

We may also obtain an expression for the clear fraction, $L_p/(L_c + L_p)$, which we call f.

$$f = (\alpha - H)/\alpha. \quad [5]$$

Equation 4 should also hold for the average dark length, l_c, and the average light length, l_p,

$$l_p = l_c(\alpha - H)/H. \quad [6]$$

If the cells are nicely separated, l_c will be a constant the size of the cell for all hematocrits. In attempting to use Eqs. 5 and 6 to analyze our data, we quickly discovered that at high hematocrits, cells are close enough together so that chains of cells appear as a single, unbroken, dark strip several cells in length. We also found that α was not constant. Thus, to Eqs. 5 and 6 we add the empirical expressions,

$$\alpha = e^{-(b_1 + b_2 H)}, \text{ and} \qquad [7]$$

$$l_c = b_3(1 + (b_4 H)^{b_5}). \qquad [8]$$

This gives us five coefficients to estimate by fitting Eqs. 5, 6, and 8 to the data for f, l_p, and l_c. We obtain l_p from the data by dividing L_p by the number of clear spaces observed. The value for l_c is calculated in an analogous manner. The differences between the logarithms to the base 10 of the observed and estimated values of f, l_c, and l_p give rise to a vector of errors, e_f, e_c, and e_p. We assume these errors to be distributed approximately as multivariate normal errors with common variance σ^2 and covariances $\rho_{ij}\sigma^2$ between e_i and e_j. We estimated the five b parameters, the covariance matrix of the errors, and the parameter covariance matrix by the method of maximum likelihood (Kendall & Stuart, 1963). Univariate least squares estimates were used in fitting models to the logarithm of the average squared clear length.

RESULTS

The use of a 400-nm broad band filter made hemoglobin appear very dark, while surrounding tissue was light. The numerical aperture of the objectives used should give a maximum resolution only slightly better than the 1/2-μm pixel spacing used. Therefore, at high hematocrits, individual red cells were usually not clearly separable, whereas at low hematocrits, individual red cells could be seen as dark spots with fuzzy edges. Gaps less than or equal to 1 μm were detected in most of our experiments at the higher hematocrits. The diameter of the vessels studied ranged from 5 to 10 μm. The rat tail showed no detectable motion due to respiration or cardiac pulsations. Axial skeletons drawn to define the center of the vessel did not usually require repositioning during a 10-second sampling period and no frame was ever rejected because of focusing changes during such a period. Successive collection periods usually did require the tracing of a new axial skeleton, but the movement amounted, at most, to tens of microns, and verification that the same vessel was being used from period to period posed no difficulty.

Of ten successive experiments, only six have been used for quantitative analysis. One experiment was rejected because hemorrhage in the field obscured our view in the middle of the experiment. Another was rejected because the coverslip was jostled, and we could not be certain of again finding the field we had begun to study. A third is omitted from our report because flow simply stopped during

the experiment. The fourth was dropped because we were unable to make cardiac output estimates or monitor and control body temperature.

One of the fields had two vessels that could be studied, so we report here on measurements made on seven capillary segments, 140 μm to 210 μm in length, obtained from six different animals. All together, we present results from 36 measuring periods at hematocrits ranging from .44 to .11.

PLASMA SPACES BETWEEN CELLS

At the beginning of the experiments, red cells filled the capillaries to the point where gaps were small and inconspicuous. As the hematocrit was lowered, the vessels appeared lighter, gaps were easily seen, and individual red cells could more often be distinguished. While all vessels followed this general scheme, quantitative measures varied greatly. This is illustrated by results from the experiment with two vessels in the same field. At the beginning of the experiment, with a systemic hematocrit of .44, the first vessel consisted of 9% plasma gap and 91% of the length darkened by red cells, with an average gap length of 3 μm. At the end of the experiment, with a hematocrit of .11, this vessel was 62% plasma with an average gap of 9 μm. The adjacent vessel began with a 3% plasma gap of 9 μm average length, and at the end was still only 27% plasma with an average gap of 8 μm.

Figure 1 shows the values of f plotted against hematocrit and the maximum likelihood estimate of f shown as a line.

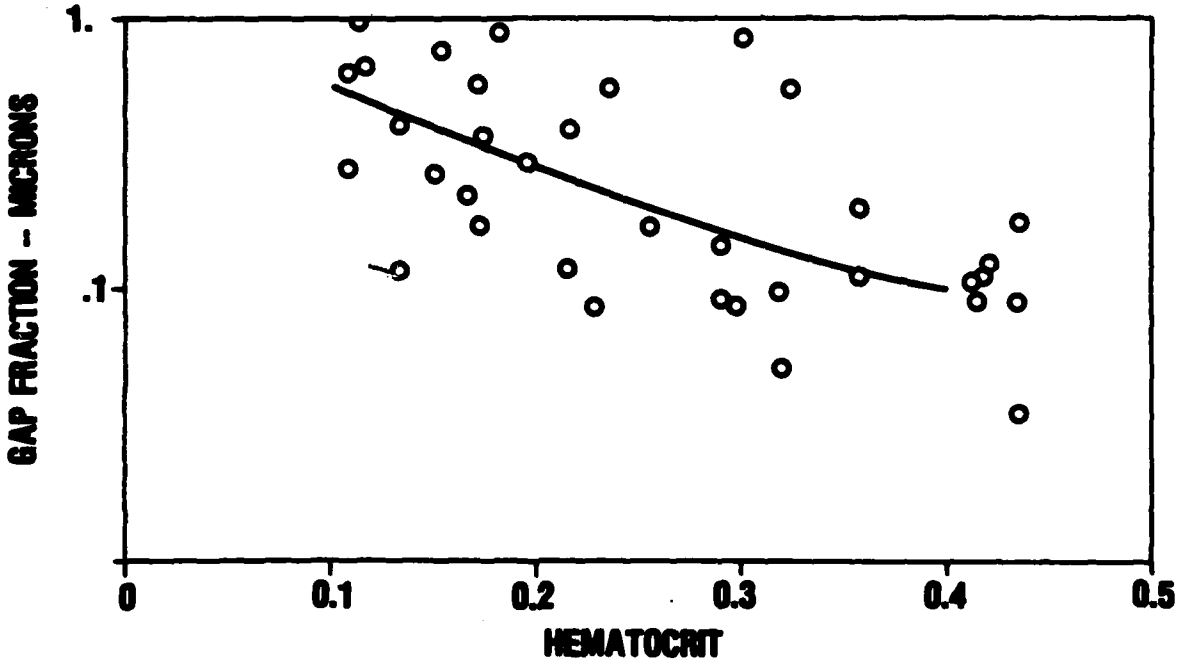

FIGURE 1. Fraction of capillary with cell-free gaps. Circles represent data points, f. The line is the maximum likelihood estimate of f based on the parameters of Table 1 and Eq. 5.

Figures 2 and 3 display similar plots for average clear lengths and average dark lengths.

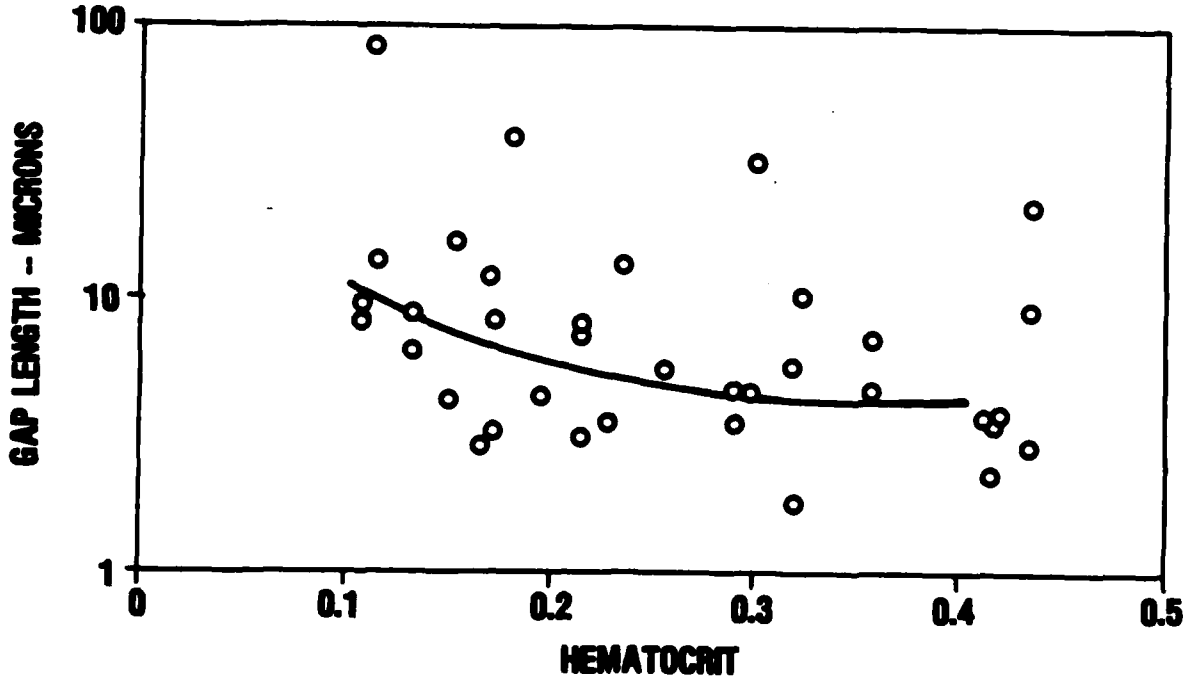

FIGURE 2. Average length of cell-free gaps. The average gap lengths measured are plotted against hematocrit. The maximum likelihood estimate of l_p (Eq. 6, Table 1) is shown as a line.

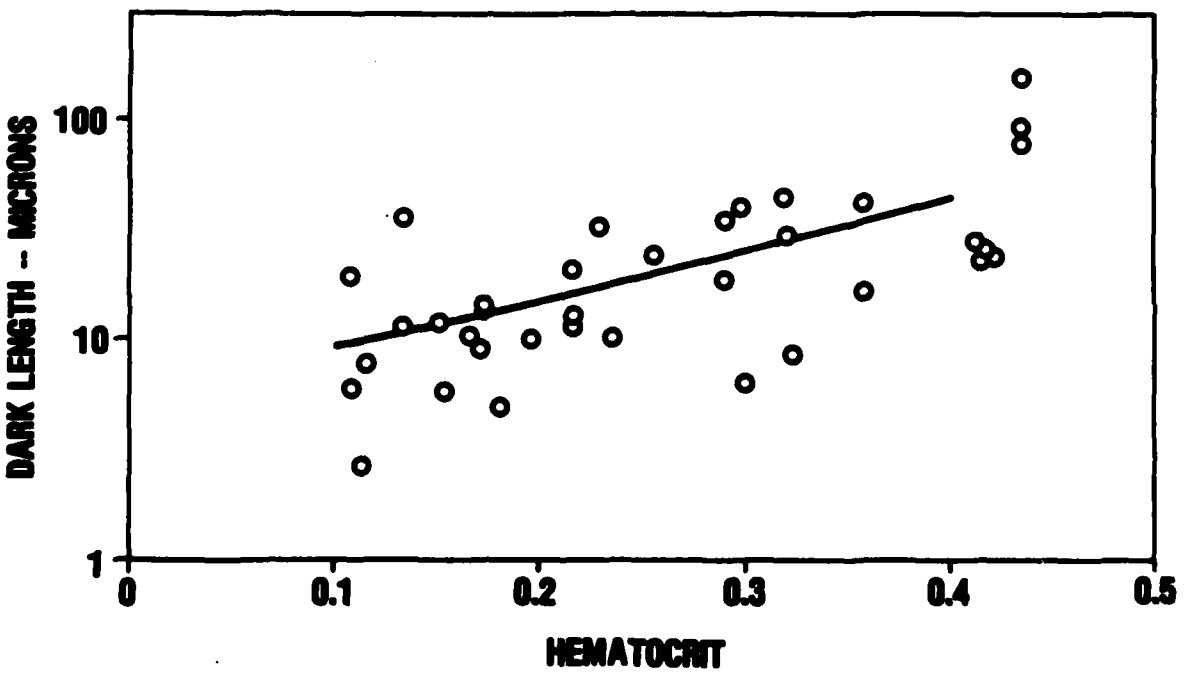

FIGURE 3. Average length of dark segments. The average length of dark capillary segments is plotted against hematocrit. The line is the maximum likelihood estimate of l_c using Eq. 8 and Table 1.

The variances for e_f, e_c, and e_p were not statistically distinguishable from one another using a likelihood ratio test (Kendall & Stuart, 1961) ($P>0.25$). The estimates from the maximum likelihood fit are shown in Table 1.

TABLE 1. Parameters of maximum likelihood estimates

b_1	1.74±.13
b_2	-2.30±.36
b_3	8.3±3.8
b_4	4.3±2.1
b_5	2.6±1.4
σ^2	.304±.033
ρ_{cf}	-.815±.077
ρ_{cp}	- .49±.16
ρ_{fp}	.68±.13

We also used a likelihood ratio test to evaluate the hypothesis that α, the average cross section occupied by a red cell, was constant. This we rejected ($P<.0001$). The hypothesis that l_c is constant rather than changing with hematocrit was also evaluated and rejected ($P<.0001$).

Table 2 shows maximum likelihood estimates for l_c, l_p, f, and α at different hematocrits.

TABLE 2. Maximum likelihood estimates and standard errors

Systemic Hematocrit	$\hat{\alpha}$	$\hat{l}_p$ μ	$\hat{l}_c$ μ	$\hat{f}$
.1	.222±.022	11.3±3.7	9.3±2.3	.549±.045
.2	.279±.018	5.56±.87	14.0±2.9	.284±.047
.3	.352±.013	4.20±.69	24.4±4.9	.146±.031
.4	.442±.014	4.44±.63	42.0±9.1	.096±.028

Also shown are estimated standard deviations for these parameters, obtained by applying propagation of error formulas with the parameter covariance matrix of the likelihood estimation. Table 2 indicates that the red cell fills almost half of its capillary cross section at a hematocrit of 0.4, but at a hematocrit of 0.1 it fills only a quarter of the available cross section. The average length of dark sections diminishes from 42 μm to about 9 μm as the hematocrit falls from 0.4 to 0.1. On the average then, these dark sections represent strings of six or seven cells at high hematocrits, but often must be single cells at low hematocrits. The fraction of the capillary occupied by clear spaces rises roughly in proportion to the change in hematocrit. To within the variability of the estimates, the clear fraction at a 0.1 hematocrit is about 4 times that at 0.4. Unfortunately, the average clear length is not determined with similar precision over the entire range of hematocrits. Between .4 and .2, however, the average clear length does not double. One simple explanation is that our method was unable to

consistently resolve spaces smaller than 1 μm, which may have been present between some of the red cells appearing unseparated. This would lead us to spuriously large estimates of l_p at high systemic hematocrits. For the purpose of calculation of an average or gradient between red cells, this would be of little importance since the gradients in such small gaps are small enough to ignore.

For the calculation of oxygen gradients in the capillary, we must know the square of the distance from the hemoglobin of the red cell. The dark lengths we assume are rich in hemoglobin. The center of long, clear spaces spaces is far from hemoglobin and should have a PO_2 lower than the PO_2 in or near the dark lengths. We name as x the distance from the center of the clear space, P_c is the oxygen partial pressure at the cell surface, and A is a tissue constant (Homer et al., 1981). The partial pressure at x is,

$$P_x = P_c + (A/2)(x^2 - (l_p/2)^2). \qquad [9]$$

At the red cell edge, $x=l_p/2$ and $P_x=P_c$. P_x is at a minimum at x=0, and may be computed using x=0 and l_p taken either from data or from our estimates of l_p or l_p^2. To compute P_x, l_p^2 is required. If l_p is constant, then the average value of l_p^2 will be the square of l_p, but if l_p is a random variable, then the square of the average of l_p will generally be smaller than the average of l_p^2. For this reason, we also did a regression of the $\log_{10}(l_p^2)$ against the $\log_{10}(b_6\hat{l}_p^2)$, where $\hat{l}_p$ was the likelihood estimate of l_p previously obtained (as shown in Fig. 4). We found $b_6=3.9\pm1.0$.

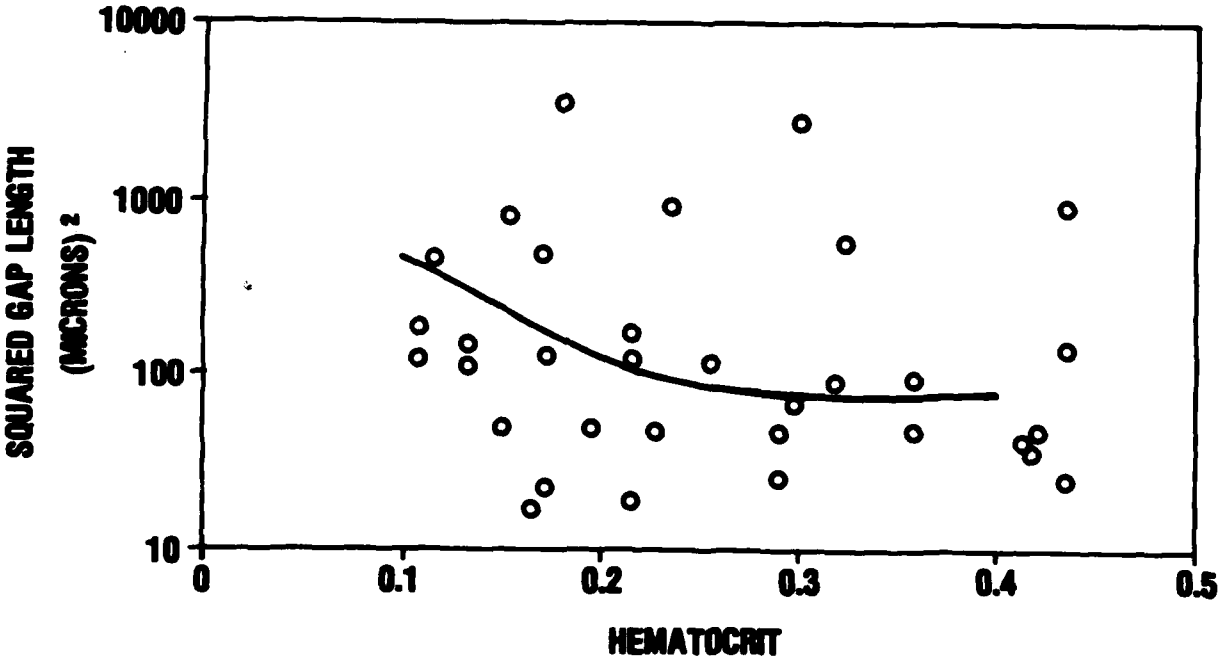

FIGURE 4. Average squared length of cell-free gaps. The average of the square of gap length is plotted against hematocrit. The line represents $3.9\,\hat{l}_p^2$, where $\hat{l}_p$ is the maximum likelihood estimate of Eq. 6.

At a hematocrit of 0.4, the average squared length was 78 μm^2. At a hematocrit of .1, the average squared length amounts to 500 μm^2. Standard deviations, in either case, are approximately 26%.

Cardiac outputs averaged .369±.010 ml/min-gm body weight at a hematocrit of 0.4, and rose about 15% to .429±.010 as the hematocrit fell to 0.1.

DISCUSSION

The preparation of shaved skin was chosen for its simplicity. It is surely not normal. Near points of bleeding, capillary stasis was often seen. A few millimeters away from points of bleeding, cell velocities calculated in a few instances were above .1 cm/sec. We searched for capillaries in these regions of high flow. These high flows possibly reflect a response to nearby injury. While capillary hematocrit has been reported to change with high flow, mass flow of cells presumably is still proportional to systemic hematocrit (Klitzman & Duling, 1979). We are not aware of other measurements of intercell spacing in acute anemia with which we might compare our results.

The parameters l_c and α are not constant but change with hematocrit. This means that if we try to fit a model to the data, assuming l_c or α or both are constant, we find that the resulting estimates of l_p tend to lie below the data points at high hematocrits and above them at low hematocrits. To correct for this, we generalized the model with which we began. The factors l_c and α depend on hematocrit, as depicted in Eqs. 7 and 8. At high hematocrits, a dark length consists of six or seven cells, whereas at low hematocrits the average dark length approaches the dimensions of a single cell. At high hematocrits, cells frequently overlap one another or are so close together we are unable to resolve them separately.

The factor α diminishes as hematocrit diminishes. This factor represents the average fraction of the capillary cross section occupied

by a length of dark hemoglobin-rich cells. Several possibilities exist to account for this. Unresolved plasma gaps would give smaller estimates of α. If these unresolved gaps were, on the average, smaller at high hematocrits than at intermediate hematocrits, we would perceive a decline in α. Genuine changes in the filling of the capillary cross section by red cells are, of course, also a possibility.

Uncertainty in the interpretation of α does not invalidate our estimates of the relationship between systemic hematocrit and observed gap sizes. Average plasma velocity in vessels less than 30 μm may be 30% lower than red cell velocity (Baker et al., 1980). Our model supposes that this discrepancy may be represented by a central plasma flow identical to red cell flow and a peripheral plasma layer that is stationary. Such a stationary layer has been suggested as an explanation for the discrepancy between small vessel hematocrits and large vessel hematocrits (Klitzman & Duling, 1979). Velocity profiles of blood flowing in glass tubes as small as 30 μm in diameter are flatter than the parabolic shape to be expected from an ideal fluid (Gaehtgens et al., 1970). Theoretical studies also indicate that flatter flow profiles are to be expected (Lew & Fung, 1970). Taken together, these papers encourage us to believe that modeling plasma flow as a core having the same velocity as red cells and a stationary peripheral layer should provide an approximation suitable to our application.

The variability in the size of gaps is great and is important to the assessment of the physiological role of cell-free gaps in acute anemia. Figure 5 shows the expected drop in oxygen tension from a cell to the center of a gap.

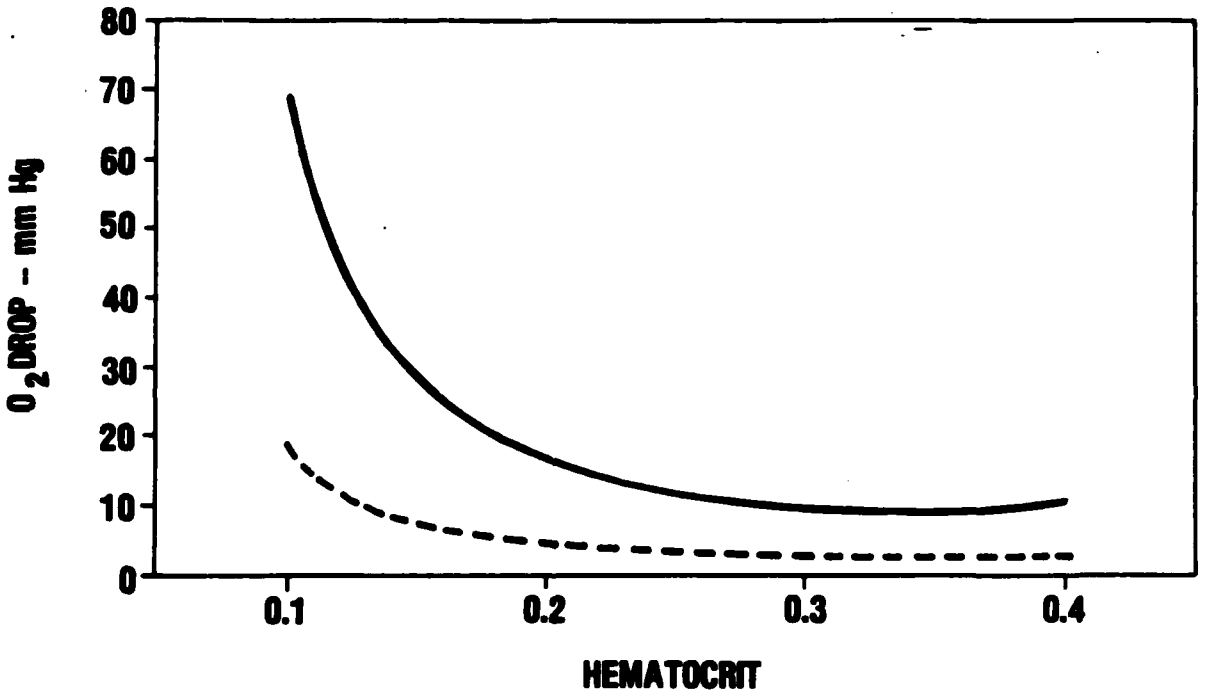

FIGURE 5. Maximum drop in oxygen tension in cell-free gaps. The lower line represents the use of the square of average l_p to Eq. 9. The top line shows the calculated O_2 drop, when the average of l_p^2 is used in Eq. 9. A was 1.1 mmHg/μ^2 for both curves (Homer et al., 1981).

The bottom curve is obtained by using the square of the average gap $(\hat{l}_p^2)$ in Eq. 9 at x=0, the center of the gap. The top curve comes from using

the average squared gap ($3.9\ l_p^2$) in Eq. 9. The difference is clearly large, and plainly agrees with one's visual impression that red cells are not evenly spaced along the capillary. With large cell-to-plasma gradients, the PO_2 in the center of the gap approaches zero and the approximation of Eq. 9 becomes poor.

A capillary with constant total plasma length, fragmented randomly into plasma gaps by a fixed number of dark segments, would be expected to have an average squared gap length just twice the size of the mean gap length squared (Homer et al., 1981). In the capillary, the total plasma length varies as does the number of intervening dark segments, so that gap sizes would be more variable than this idealization. The observed ratio of the average squared gap length to the square of the average gap length was 3.9±1.0. This ratio is about what one would expect if the gaps were randomly distributed, with a tendency towards some greater number of very small and very large gaps than would arise from a perfectly uniform distribution of gap sizes. This great variability in gap sizes means that even at hematocrits of .4, gaps large enough to harbor PO_2 gradients of 20 mm Hg would not be rare. Consider a capillary segment 200-μm long with 0.1 of its length occupied by plasma gaps as predicted for a hematocrit of 0.4. With an average gap length of 4.4 μm, we would expect a random snapshot of this capillary to contain, on the average, 4 or 5 plasma gaps. Taking into account the variability in l_p, we would expect about 15% of the gaps to exceed 12 μm, and hence have a mid-gap PO_2 about 20 mm Hg lower than the

enclosing cells. Somewhere between one-half and one-third of our snapshots would contain such a gap. Calculations of this sort are not affected by our failure to detect small gaps between strings or red cells at high hematocrits. The frequency of large gaps (and transient low PO_2s) expressed in this way does not depend on undetected small gaps. Average capillary PO_2s also may be calculated from our data with little distortion because of the undetected small gaps. The average PO_2s will be the sum of the average calculated from Eq. 9 and our data multiplied by the detected gap fraction, plus red cell PO_2 multiplied by red cell fraction, plus undetected gap PO_2 multiplied by undetected gap fraction. But the PO_2s in small undetected gaps will be the same as for red cells and, hence, inclusion of these gaps with the cell fraction will not alter the calculated average capillary PO_2.

The variable size of the gaps might be thought to contribute to the great scatter observable in Figs. 1 through 5, and indeed it must. In magnitude, however, we have calculated that the greater portion of the scatter seen in these figures arises from some other source. The distribution of gap sizes varies from capillary to capillary. Some of this may be variation from time to time, or variation between capillaries in different places, or even variability between animals. Our experiments were not designed to sort out these possibilities.

With new optical techniques for the measurement of PO_2s in cells, gradients greater than 20 mm Hg should be detectable (Benson et al.,

1980). The increase in average gap size with decrease in hematocrit proved to be less than we had expected (Homer et al., 1981), but still large enough to provide potentially detectable oxygen gradients. The physiological significance of such gradients, if indeed they exist, is harder to assess. As described previously, they may account for the fact that in acute anemia, hemoglobin solutions with P50s well below that of the red cells still are effective in delivering oxygen to tissues (Moss et al., 1976). We had not previously considered that oxygen gradients in plasma gaps were likely to be of any importance in the delivery of oxygen to tissues at normal hematocrits, but the great variability in gap size means that the endothelial wall may be exposed to brief, but fairly frequent, sudden drops in PO_2. It is difficult for us to believe that these transients can be of much direct importance in the delivery of oxygen, but they could provide regulatory signals. A given endothelial cell would be exposed to pulses of O_2 changes, whose frequency, magnitude, and duration might condition the release of metabolites signaling for some modification of these factors. In any case, if the existence of such gradients at normal hematocrits were to be confirmed, we should certainly be obliged to invent this or some other purposeful explanation for such an interesting observation.

REFERENCES

Baker, C. H., E. T. Sutton, and D. L. Davis. Microvessel mean transit time and blood flow velocity of sulfhemoglobin-RBC. Am. J. Physiol. 238:H745-749, 1980.

Benson, D. M., J. A. Knopp, and I. S. Longmuir. Intracellular oxygen measurements of mouse liver cell using quantitative fluorescence video microscopy. Biochim. Biophys. Acta 591:187-197, 1980.

Gaehtgens, P., H. J. Meiselman, and H. Wayland. Velocity profiles of human blood at normal and reduced hematocrit in glass tubes up to 130 μ diameter. Microvasc. Res. 2:13-23, 1970.

Homer, L. D., P. K. Weathersby, and L. A. Kiesow. Oxygen gradients between red blood cells in the microcirculation. Microvasc. Res. 22:308-323, 1981.

Kendall, M. G., and A. Stuart. The Advanced Theory of Statistics. Vol. 1, Distribution Theory. New York: Hafner, 1963.

Kendall, M. G., and A. Stuart. The Advanced Theory of Statistics. Vol. 2, Inference and Relationship. New York: Hafner, 1961.

Klitzman, B., and B. R. Duling. Microvascular hematocrit and red cell flow in resting and contracting striated muscle. Amer. J. Physiol. 237:H481-H490, 1979.

Lew, H. S. and Y. C. Fung. Plug effect of erythrocytes in capillary blood vessels. Biophys. J. 10:80-99, 1970.

Moss, G. S., R. Dewoskin, A. L. Rosen, H. Levine, and C. K. Palani. Transport of oxygen and carbon dioxide by hemoglobin-saline solution in the red-cell-free primate. Surg. Gynecol. Obstet. 142:357-362, 1976.

GPO 909-884

END

FILMED

9-85

DTIC